2019-09-01

# Microfluidics-based four fundamental electronic circuit elements resistor, inductor, capacitor and memristor

Goran Stojanović, Milivoj Paroški, Nataša Samardžić, Milan Radovanović, Dejan Krstić

electronics

MDPI

Article

# Multi-layered microfluidics-based four fundamental electronic circuit elements R, L, C and M

**Goran Stojanović[1,*], Milivoj Paroški[1], Nataša Samardžić[1], Milan Radovanović[1], Dejan Krstić[1]**

[1] University of Novi Sad, Novi Sad, Serbia
* Correspondences; sgoran@uns.ac.rs

Received: date; Accepted: date; Published: date

**Abstract:** The microfluidics domain has been progressing rapidly recently, particularly considering its useful application in the field of biomedicine. This paper presents a novel, microfluidics-based design for four fundamental circuit elements in electronics, namely, resistor, inductor, capacitor and memristor. These widely used passive components were fabricated using a precise and cost-effective xurography technique, which enables the construction of multi-layered structures on foil, with gold used as a conductive material. To complete their assembly, an appropriate fluid was injected into the microfluidic channel of each component: the resistor, inductor, capacitor and memristor were charged with transformer oil, ferrofluid, NaCl solution and $TiO_2$ solution, respectively. The electrical performance of these components was determined using an Impedance Analyzer and Keithley 2410 High-Voltage Source Meter instrument and the observed characteristics are promising for a wide range of applications in the field of microfluidics electronics.

**Keywords:** microfluidics; xurography; resistor; capacitor; inductor; memristor

## 1. Introduction

It is well known that the four fundamental two-terminal circuit elements in electrical engineering are the resistor (R), inductor (L), capacitor (C) and memristor (M) [1]. These four basic elements can be described using the following variables: electric current $i$, voltage $v$, charge $q$ and magnetic flux $\varphi$ [2]. There are many published papers describing methods to manufacture these components in conventional electronics or in microelectronics, using various fabrication technologies. In microelectronics, these components are usually rigid and have a static geometrical shape.

In previous decades, the field of microfluidics has been developing and growing rapidly, primarily thanks to a wide range of applications in biomedicine. Nevertheless, microfluidics can also have useful applications in electronics, bearing in mind that microfluidics-based electronics can provide flexible and transparent components [3]. While the use of fluids and gels in the construction of various electronic devices has been demonstrated previously as reviewed below, to the best of our knowledge, literature reports demonstrating uniform fabrication techniques for microfluidic versions of the four passive electronic components are lacking.

The measurement of microfluidic channel electrical resistance was demonstrated in [4] on a Polydimethylsiloxane (PDMS) microfluidic device. Nine different designs were fabricated, twenty-seven devices were tested and a correlation between electrical resistance and fluidic resistance was established. In [5], the authors reported the use of a 3D printer and laser for manufacturing inductors and transformers of different shapes. They applied liquid conductive (galinstan) and magnetic (commercial ferrofluid) materials, achieving a maximum quality factor (Q-factor) value equal to 71. Banitorfian et al. [6] presented a structure in the form of a solenoid from copper wire mounted on a printed circuit board (PCB), through the middle of which a ferrofluid-filled tube was inserted. The volume of the ferrofluid in the tube regulated the penetration of the magnetic field along the length of the solenoid, and in that manner a variable inductor was achieved. However, this solution

combined different manufacturing techniques which are not automated and it is not possible to obtain a compact electronic component. Elsewhere, a microfluidic chip featuring a channel going through the middle of a 0.025-mm-diameter copper wire coil was reported [7], but was limited to a sensor application. The coil was created in the form of a solenoid with 600 turns and the internal diameter of the air-cored coil was 0.3 mm. A total inductance around 42.9 nH was obtained. The same author presented a similar inductive sensor application using a single layer planar coil with a diameter of 50 μm made from 33 turns of copper wire [8]. The diameter of the microchannel was 270 μm, resulting in a total inductance of 1.25 μH.

Various capacitors featuring liquids have also been reported. For example, a ring-shaped plate capacitor was reported in [9], not as a separate component, but to function as a relative permittivity sensor. The fluid-filled channel in the sensor was lying perpendicular to the direction of the electrical conductors and pads. In another example [10], the main idea of the authors was to modify the radio frequency (RF) characteristics of a microwave capacitor, fabricated using photolithography, and including spiral-shaped, deionized water-filled capacitor electrodes. In this way, the authors succeeded to increase capacitance from 0.52 pF to 18.5 pF when the channel was empty or filled, respectively, in the frequency range from 0.1 to 4 GHz. The same group of authors described a similar principle in [11], for a continuously tuned capacitor. An interdigitated capacitor with a PDMS microreservoir of fluid on top of the structure was presented in [12]. This device changed capacitance from 10 pF (in air) to 50 pF (in deionized water). In another report, a liquid metal (GaInSn) - liquid dielectric (silicone oil, glycerol, or water) capacitor structure was created using PDMS as a base material [13]. The capacitor was composed of two cylindrical electrodes and obtained capacitance up to 10 pF depending on the gap between the electrodes and incorporated material. Further, a parallel plate capacitor and a planar spiral inductor were presented in [14], creating a wireless biosensor with a microchannel inside the LC structure, fabricated in Low Temperature Co-fired Ceramics (LTCC) technology. The resonant frequency was changed with variation of the permittivity of the liquid in the microchannel in the LTCC structure. Another microfluidic device with a straight microchannel and two embedded single-layer inductance coils as well as a micro capacitor was reported in [15], using PDMS and applied for the detection of contamination in hydraulic oil.

In accordance with the general trend of creating all-soft-matter components and circuits [12], a prototype of quasi-liquid memristors was presented in [16]. The device was composed of hydrogel layers doped with polyelectrolytes as an active material, with liquid metal electrodes [16]. A change in the overall resistive state was achieved in accordance with the local change of pH in the gel. Furthermore, a fluidic memristor can also be designed to exhibit sensing properties using indium tin oxide (ITO) glass as substrate and bottom electrode, a $TiO_2$ layer representing the active film, PDMS for the inlet and outlet chamber of the chip and Al top electrode [17]. Sensing functions were realized through nine wells, each with a diameter of 1 mm, which acted as a liquid position area, allowing the device to detect the concentration of D-GLucose by measuring I-V characteristics and $R_{off}$-$R_{on}$ ratios. The manufacturing of a nanofluidic memristor suitable for use as a core element in neuromorphic computing within flexible devices was proposed in [18]. A track-etching technique was used to form a conical nanochannel (minimum diameter of 6 nm) which was responsible for the hysteretic loop in the I-V curve as the positive bias voltage created a depletion state within the channel, which was filled with IL (ionic liquid)/water solution [18]. From previously described state-of-the-art analysis in the field, it is obvious that there is a need for cost-effective, rapid prototyping technology which can be used for fabrication of all four fundamental elements. This paper addresses this challenge.

We here present the design, fabrication and characterization of four fundamental circuit elements – R, L, C, and M. These components were fabricated using a rapid prototyping xurography technique, which is based on creating the different geometrical shapes of components in PolyVinyl Chloride (PVC) foils and laminating them under elevated temperature and pressure. Gold leaves were used as a conductive material and after cutting separate layers in the desired pattern, multi-layered compact electronic structures were obtained. Electrical parameters were determined for all fabricated components, using impedance spectroscopy and I-V measurements. Resulting

performances were better or comparable with previously published reports of components manufactured using sophisticated and costly technologies.

## 2. Materials and Methods

Four components presented in this paper were fabricated using a very precise xurography technique. Xurography is a rapid prototyping computer controlled method which employs a knife plotter to create microstructures of different geometries into thin foils or layers. It enables lamination of multi-layered structures mechanically carved from pressure sensitive and thermal activated adhesive foils in a very short period of time, without the necessity for costly clean room facilities.

### 2.1 Resistor design

The resistors were composed of three layers. The substrate was PVC foil, on which the gold electrodes for contacts were glued. The middle layer was formed from foil and contained the microfluidic channels. We designed three types of resistors in the meander shape, creating different length channels (10 mm, 15 mm and 20 mm in the x axis) to provide varying values of resistance. The top layer, also of PVC foil, contained the inlet, outlet and contact pads. The design of the complete structure is illustrated in Figure 1(a) and one of the fabricated microfluidic resistors is shown in Figure 1(b). The total dimensions of this structure are 5 cm × 2 cm. For the purpose of testing these resistors we used liquid dielectric materials – transformer oils and synthetic oil. Figure 2 shows carved separate layers of PVC foils. The width of the microfluidic channel was 1 mm, whereas the diameter of the holes was 2 mm.

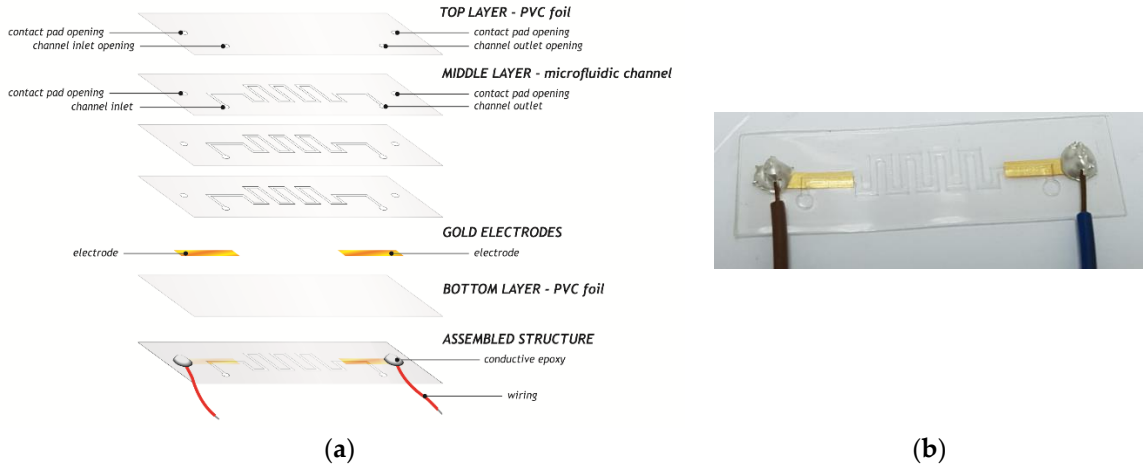


**Figure 1.** (**a**) Design of multi-layered resistor, (**b**) one of the fabricated microfluidic resistor.

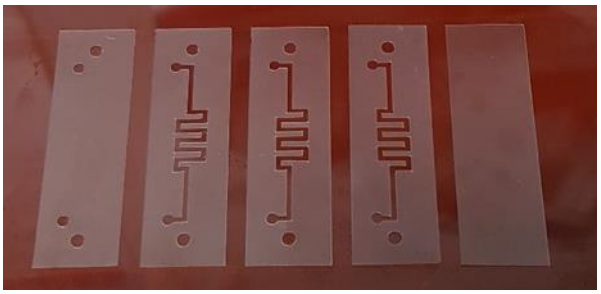

**Figure 2.** Separate layers of PVC foils.

### 2.2 Inductor design

The inductor was designed in the solenoid form with 7 turns. The Autocad software package was used for drawing patterns for each layer. The xurography technique uses a cutter plotter to mechanically cut each layer of the solenoid structure in PVC foil. Graphtech pro studio software was

used to control the cutting process using a computer and the cutter plotter. The complete structure was composed of 5 layers. At the bottom, PVC foil was used as a substrate. After that came a layer incorporating the bottom part of the solenoid electrode structure. The middle layer contained a microfluidic channel for injection of ferrofluid (liquid magnetic material) which exactly represents the solenoid core, in order to increase the total inductance of the proposed structure. The dimensions of the channel were 4 cm × 0.8 cm. The fourth layer included the upper part of the conductive electrodes. Finally, the fifth layer contained holes for inlet and outlet of fluid as well as pads for connecting wires from each terminal of the solenoid structure. Conductive gold segments in the second and fourth layer were electrically connected with silver paste. The design of all layers is shown in Figure 3(a), whereas Figure 3(b) depicts the complete fabricated inductive structure.

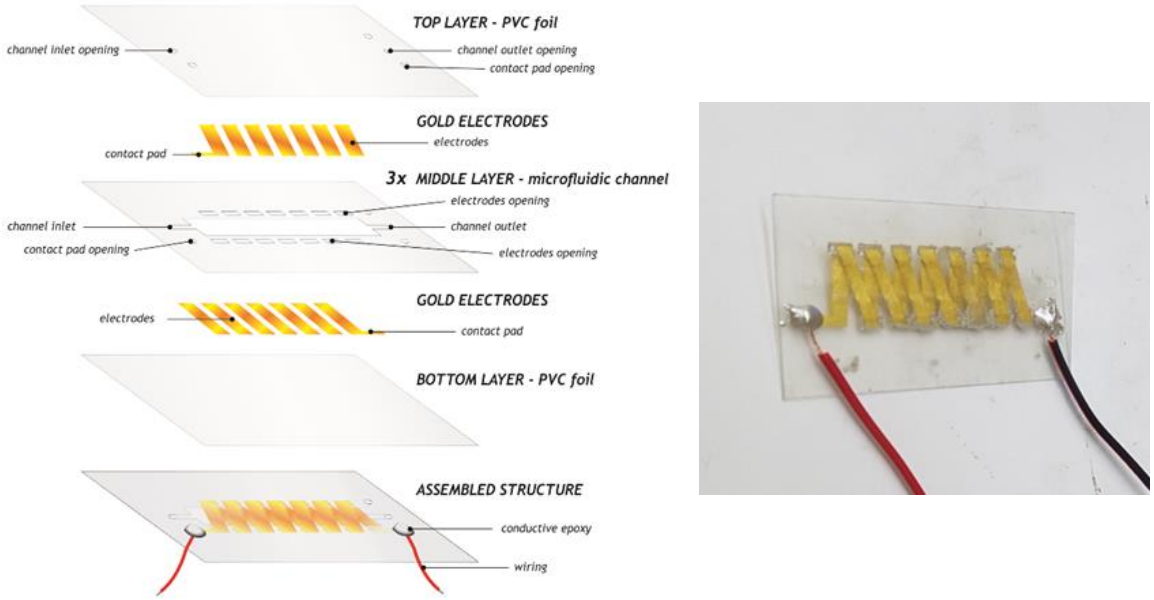


(**a**) (**b**)

**Figure 3.** (**a**) Design of all layers of the inductive structure, (**b**) fabricated solenoid inductor.

The separate layers for fabrication of solenoid inductor, cut in PVC, and gold conductive segments can be seen in Figure 4. We used foils with thickness of 80 μm. Each conductive segment had dimensions of 2.5 mm × 15 mm. The thickness of the gold segments was around 10 μm. Separate layers were stacked and laminated together using a laminator at 130 °C and the fabricated two-terminals inductor is shown in Figure 3(b). The total dimensions of this microfluidic inductor were 5.5 cm × 3.6 cm.

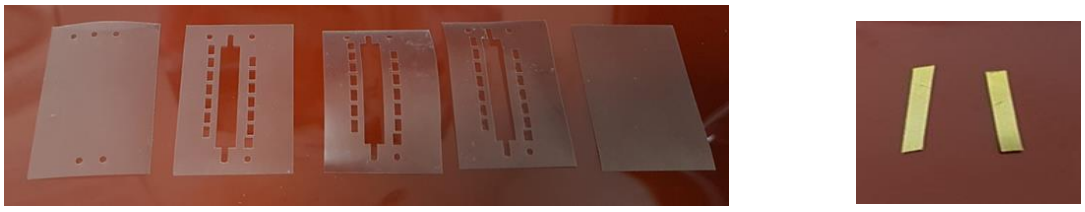

(**a**) (**b**)

**Figure 4.** (**a**) Separate layers of PVC foil for inductor fabrication, (**b**) conductive segments for solenoid turns.

### 2.3 Capacitor design

We designed a parallel plate capacitor with two gold electrodes, between which is the space for the microfluidic channel, filled afterwards with liquid dielectric. The fabricated structure is presented in Figure 5, whereas the separate layers can be seen in Figure 6. The capacitor is composed of five layers. The bottom PVC foil layer has a role of substrate and a contact from the bottom electrode of the capacitor is created on this layer. The next layer consists of the electrode. In the middle layer, the

microfluidic channel was created. The fourth layer is comprised of the second plate electrode and finally the fifth layer is for the inlet, outlet and contact for the second electrode. The dimensions of the gold electrodes are 4 cm × 2 cm and the total dimensions of the fabricated structure are 5 cm × 3 cm. The distance between electrodes is equal to the thickness of one PVC foil, which is around 80 µm.

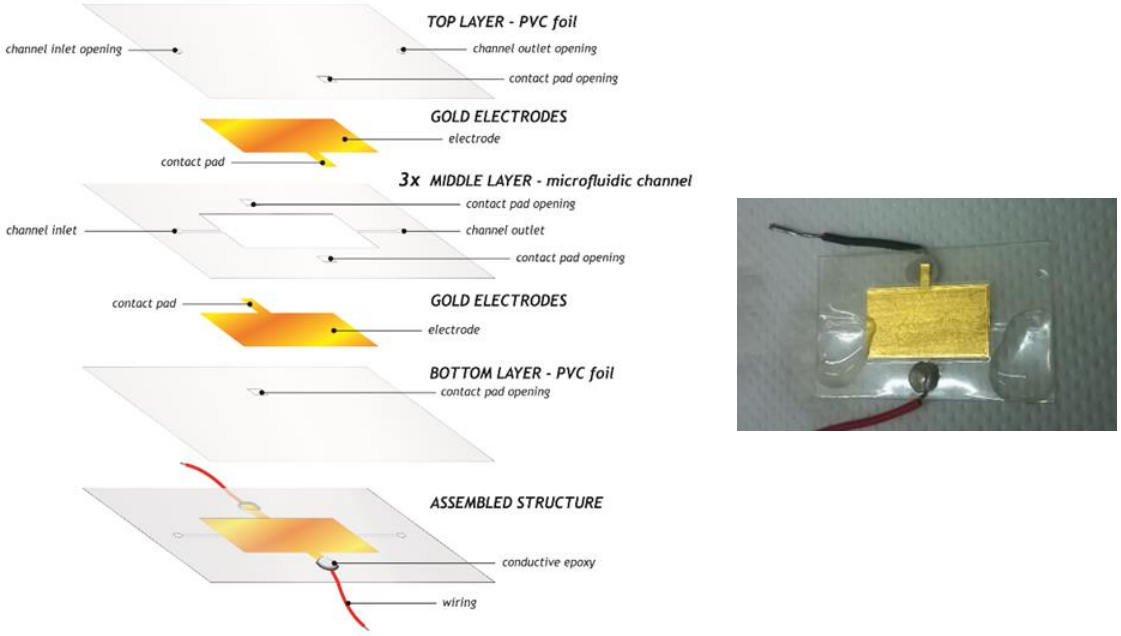


(**a**) (**b**)

**Figure 5.** (**a**) Design of all layers of the capacitive structure, (**b**) fabricated microfluidic capacitor.

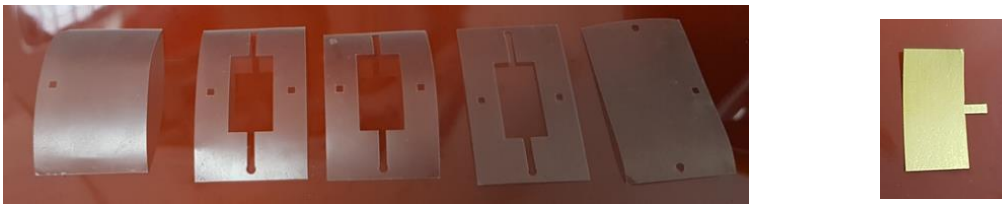

(**a**) (**b**)

**Figure 6.** (**a**) Separate layers of microfluidic capacitor, (**b**) electrodes for parallel plate capacitor.

## 2.4 Memristor design

The memristor is designed similarly to the resistor, but with a straight microfluidic channel. We analyzed the device with the length of the channel equal to 5 mm, and width of 1.4 mm. As a typical active material for memristors is $TiO_2$, we used $TiO_2$ nanopowder (as a 1% solution) and injected this solution into the microfluidic channel using a syringe. Figure 7 depicts the appearance of the fabricated memristor with 5 mm channel length. The total dimensions of the fabricated memristors were 5 cm × 2 cm.

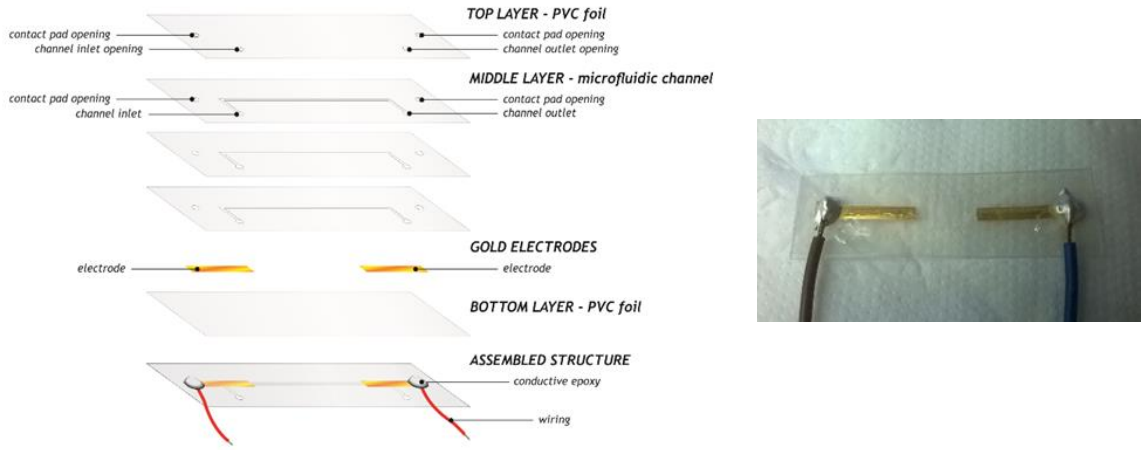


(**a**) (**b**)

**Figure 7.** (**a**) Design of all layers of the memristive structure, (**b**) fabricated microfluidic memristor.

## 3. Results and Discussion

For testing the described components, we used an Impedance analyser HP4149A as well as Keithley 2410 High-Voltage Source Meter controlled with the LabVIEW platform. Part of the experimental setup can be seen in Figure 8.

(**a**) (**b**)

**Figure 8.** Experimental set-up with: (**a**) Impedance Analyzer HP4194A for testing R, L and C, (**b**) Keithley 2410 for testing M.

The three types of fabricated resistors were tested through the injection of transformers oil as a liquid material into the meander-shaped microfluidic channel. The measured resistance for these three cases of different length channels are presented in Figure 9. From Figure 9 can be concluded that resistance is increased with increasing the length of the channel, which is in accordance with the equation: $R = \rho l/A$, where $\rho$ is the resistivity of the applied dielectrics, $l$ is the length of the microfludic channels and $A$ is the surface area (width of the channel × thickness of the channel). The total lenght of the channels for three types of fabricated structures were: 28, 42, and 62 mm. Transformer oil has higher resistivity than synthetic (motor oil) and as a consequane higer resistance value for the same channel length.

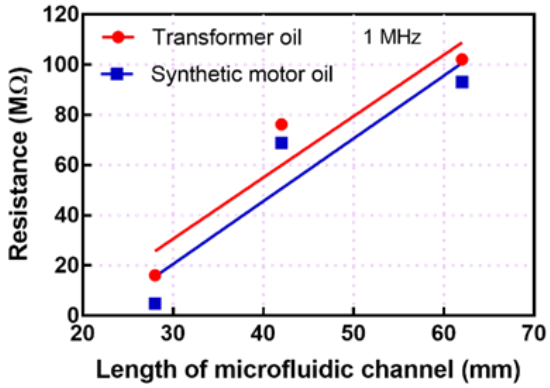


**Figure 9.** Resistance as a function of the channel length for transformer oil and synthetic motor oil as resistive materials.

For the inductor we studied the solenoid structure to achieve the best coupling between coils, which would result in higher mutual inductance and, consequently, higher total inductance of the component. In the channel, the liquid magnetic material – ferrofluid, was injected in order to additionally increase the total inductance, according to the following expression $L = \frac{AN^2\mu_0\mu_r}{l}$, where $A$ is cross-section area, $N$ is number of turns, $\mu_0 = 4\pi 10^{-7}\frac{N}{A^2}$ is the permeability in vacuum, $\mu_r$ is the relative permeability of ferrofluid and $l$ is the length of the channel equal to 4.5 cm.

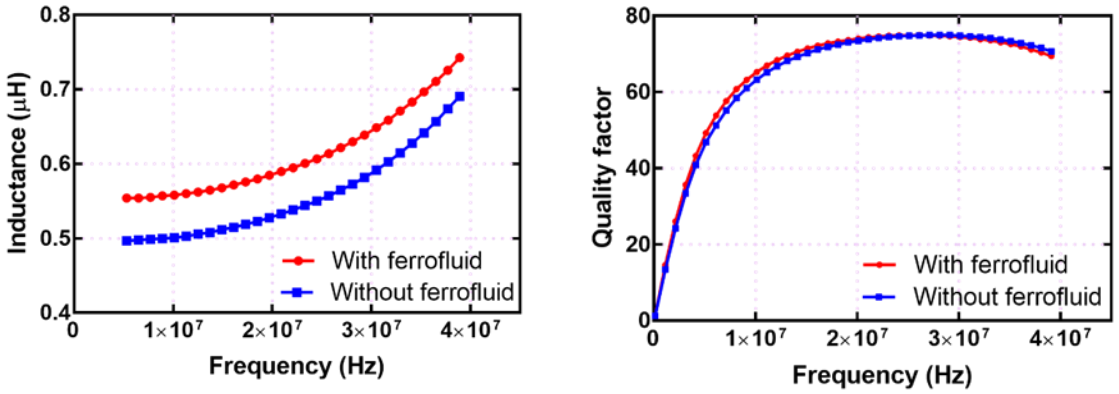


(**a**) (**b**)

**Figure 10.** Experimental set-up with: (**a**) Impedance Analyzer HP4194A for testing R, L and C, (**b**) Keithley 2410 for testing M.

The measured inductance and quality factor, without and with ferrofluid inside the channel, are presented in Figure 10. The total inductance is around 500 nH at the frequency of 10 MHz with an empty channel, whereas this value is equal to 560 nH with ferrofluid material inside of the channel, having the role of the liquid core for the solenoid. This is approximately a 12% increase in the total inductance. The advantage of our approach is that this increase in total inductance is not paid by increasing the weight and size of the component, which is usually the case in conventional ferrite-based inductors and transformers. The most bulky part of the inductive components in classical electronics is the magnetic core. On the contrary, in microfluidics-based electronics we used a very small amount of liquid and the weight of the component changed can be measured in μg. The maximum value obtained for the quality factor was 75 at a frequency equal to 26 MHz. This maximum value was higher than the value published in [5], which was 71.

To test the capacitor, a solution of NaCl in different concentrations was injected into the microfluidic channel. In this way, the dielectric constant of the parallel plate capacitor was increased according to the formula $C = \frac{\varepsilon_0\varepsilon_r A}{d}$, where $\varepsilon_0 = 8.85 \times 10^{-12}\frac{F}{M}$, $\varepsilon_r$ is the relative permittivity of dielectric inside of the channel, $A$ is the surface area of electrodes and $d$ the distance between them.

Measured capacitance as a function of frequency for different concentration of NaCl as a parameter is shown in Figure 11. A higher concentration was associated with a higher dielectric constant and increasing capacitance. Measured capacitance decreased with increasing frequency, bearing in mind that the same trend has a dielectric constant, due to different types of polarization which can be noticed from low frequencies towards the high frequency range.

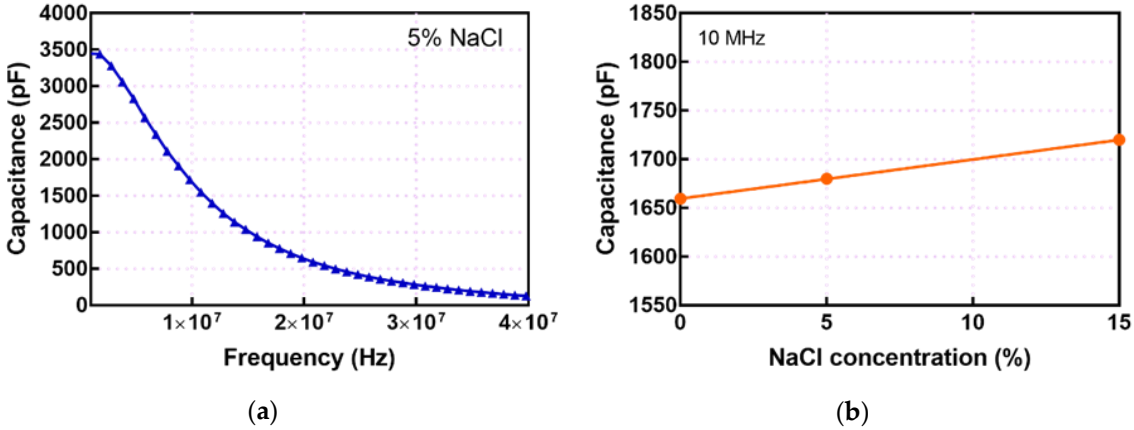


(**a**) (**b**)

**Figure 11.** Capacitance of microfluidic capacitor as a function of: (**a**) frequency for 5% NaCl solution, (**b**) different concentration of NaCl solution inside the channel.

For memristors, a solution of $TiO_2$ nanopowder (1 %) was prepared and injected into the straight line shaped microfluidic channel. Measurements were performed using Keithley 2410 High-Voltage Source Meter controlled with the LabVIEW platform (ambient conditions, temperature $\sim$ 300 $K$). The actuation voltage was a bipolar voltage waveform (0 V $\rightarrow V_{max} \rightarrow$ 0 $\rightarrow$ -$V_{max} \rightarrow$ 0 V), triangular waveform, with a sweep speed of 1 V/ms and voltage amplitude of 20 V. Ground (referent) potential is connected to the microfluidic device inlet, while positive voltage is connected to the device's outlet, Figure 8(b). Measurement results are shown in Figure 12. Transition from High Resistive State (HRS)/ON state to Low Resistive State/OFF state occurs for negative voltage polarity at $\sim -20$ V. The obtained hysteresis loop in I-V characteristic (determined by the direction of switching), belongs to the non-crossing type (NCT), or tangential hysteresis loop, i.e. two parts of the loop only touch each other, and do not intersect, [19]. According to measured results, presented in Figure 12, we estimated OFF-to-ON resistive ratio around a factor of 2. Unlike other reported results in the literature for microfluidic memristors, [16]-[18], current-voltage characteristicsof the fabricated device exhibits hysteresis for both positive and negative polarities of actuation voltage, consequently it represents a bipolar class of resistive switching devices. Furthermore, existing loops in the 1st and 3rd quadrants of the I-V plane show similar lobe area (close to symmetric loops), which indicates low dissipation, i.e. lower Joule heating compared to results reported in the literature, [16]-[18].

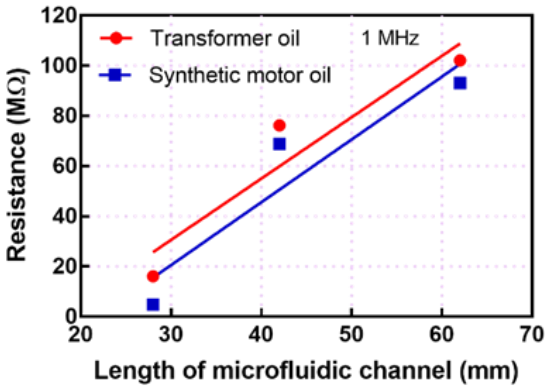


**Figure 12.** I-V characteristics of fabricated microfluidic memristor.

This observation can be explained by the symmetric structure of the device as well as low-Ohmic contact between electrodes achieved by the combination of Au electrodes and silver paste contacts between the device and the wires.

## 4. Conclusion

In this work we have connected the fields of microfluidics and electronics, presenting the design, fabrication and testing of four fundamental circuit elements, R, L, C, and M, the characteristics of which are improved by injecting the appropriate fluid into the microfluidic channels. We applied a precise, rapid prototyping xurography technique, enabling fabrication of robust, mechanically flexible, transparent and lightweight components. This method enables the manufacture of electronic components very rapidly, using cost-effective equipment and without a requirement for clean room facilities. The proposed components will further advance the development of the electronics and microfluidics industries as well as could have potential to make revolutionary changes in the field of passive electronic components.

**Author Contributions:** Investigation, Milivoj Paroški, Nataša Samardžić and Milan Radovanović; Methodology, Goran Stojanović; Resources, Goran Stojanovic; Visualization, Dejan Krstić; Writing – original draft, Goran Stojanović, and Nataša Samardžić.

**Acknowledgments:** Results presented in this article received funding from the European Union's Horizon 2020 research and innovation programme under the Marie Skłodowska-Curie grant agreement no. 690876 – MEDLEM as well as being partly supported within project no. III45021.

**Conflicts of Interest:** The authors declare no conflict of interest.

## References

1. Shan S.D., Sheng C.Y., Xian C.Z., Jun L., Young S. Toward the complete relational graph of fundamental circuit elements, *Chin. Phys. B* **2015,** *Volume* 24, 068402.
2. Strukov D.B., Snider G.S. Stewet D.R, Williams S. The missing memristor found, *Nature* **2008,** *Volume* 453, 06932.
3. Cheng S., Wu Z. Microfluidic electronics, *Lab on a chip* **2012**, 2lc21176.
4. Godwin. L.A, Deal K.S, Hoepfner L/D/, Jackson L.A., Easley C.J. Measurement of Microchannel Fluidic Resistance with a Standard Voltage Meter, *Anal Chim Acta.* **2013**, *Volume* 758, pp. 101–107.
5. Lazarus N., Bedair S.S., Smith G.L. Creating 3D Printed Magnetic Devices with Ferrofluids and Liquid Metals. *Additive Manufacturing* **2019**, *Volume* 26, pp. 15–21.
6. Banitorfian, F., Eshghabadi, F., Manaf, A.A., Noh, N.M., Mustaffa. M.T. A Novel Ferrofluids-Based High-Tuning High-Q Variable Solenoid Inductor for Frequency-Reconfigurable Circuits Applications, *IEEE International Circuits and Systems Symposium (ICSyS)*, 2-4 Sept. 2015.
7. Wu Y. Detection of foreign particles in lubrication oil with a microfluidic chip, *Industrial Lubrication and Tribology* **2018**, *Volume* 70, pp. 1381–1387.
8. Wu Y., Zhang H. Research on the effect of relative movement on the output characteristic of inductive sensors, *Sensors and Actuators A* **2017**, *Volume* 267, pp. 485–490.
9. Andersson M., Wilson A., Hjort K., Klintberg L. A microfluidic relative permittivity sensor for feedback control of carbon dioxide expanded liquid flows, *Sensors and Actuators A* **2018**, *Volume* 11, 015.
10. Habbachi N., Boussetta, H., Boukabache, A., Kallala, M.A., Pons, P., Besbes K. Fabrication and modelling of a capacitor microfluidically tuned by water, *IEEE Electron Device Letters* **2016**; *Volume* 38, 16619845.
11. Habbachi N., Boussetta H., Boukabache A., Kallala M.A., Pons P., Besbes K. Design and fabrication of a continuously tuned capacitor by microfluidic actuation, *J. Micromech. Microeng.* **2018**, *Volume* 28, 035012.
12. Kim M.G., Alrowais, H., Pavlidis S., Brand O. Size-Scalable and High-Density Liquid-Metal-Based Soft Electronic Passive Components and Circuits Using Soft Lithography, *Adv. Funct. Mater.* **2016**, *Volume* 27, 201604466.

13. Liu S., Sun X., Hildreth O.J., Rykaczewski K. Design and characterization of a single channel two-liquid capacitor and its application to hyperelastic strain sensing, *Lab on a chip* **2015**, *Volume* 15, pp. 1376–1384.
14. Liang Y., Ma M., Zhang F., Liu F., Liu Z., Wang D., Li Y. An LC Wireless Microfluidic Sensor Based on Low Temperature Co-Fired Ceramic (LTCC) Technology, *Sensors* **2019**, *Volume* 19, E1189.
15. Zeng L., Zhang H., Zhao H., Yu Z., Teng H. Novel Inductance/Capacitance Microfluidic Chip for the Multi-Contamination Detection in Marine Hydraulic Oil, *Prognostics and System Health Management Conference (PHM-Harbin)* **2017**.
16. Koo H.J., So J.H., Dickey M.D., Velev O.D. Towards All-Soft Matter Circuits: Prototypes of Quasi-Liquid Devices with Memristor Characteristics, *Adv Mater.* **2011**, *Volume* 16, pp. 3559–3564.
17. Hadisa M.N.S., Manafa A.A., Ngalimc S.H., Hermand S. H. Fabrication and characterisation of fluidic based memristor sensor for liquid with hydroxyl group, *Sens Biosensing Res.* **2017**, *Volume* 14, pp. 21–29.
18. Sheng Q., Xie Y., Li J., Wang X., Xue J. Transporting ionic-liquid/water mixture in a conical nanochannel: a nanofluidic memristor, *Chem. Commun.* **2017**, *Volume* 53, pp. 6125–6127.
19. Biolek Z., Biolkova D., Biolkova V., Kolka Z. Comments on Pinched Hysteresis Loops of Memristive Elements, *Radioengineering* **2015**, *Volume* 24, pp. 962–967.